Forschungszentrum Karlsruhe
in der Helmholtz-Gemeinschaft

Forschungszentrum Karlsruhe GmbH, Institut für Materialforschung I
P.O. Box 36 40, 76021 Karlsruhe, Germany
M. Rieth, M. Klimiankou, E. Materna-Morris

A Steady-State Creep Model for the AISI 316 L(N) in the Technically Relevant Stress Range

Among many other applications the austenitic 17/12/2–CrNiMo steel 316 L(N) (DIN 1.4909) is used or envisaged for both conventional and nuclear power plant construction as well as for ITER within the International Nuclear Fusion Project. Worldwide a huge number of experimental investigations have already been carried out to determine the material properties (including creep behavior) of this steel type in the conventional stress and temperature range. In the design relevant low-stress range at 550 °C and 600 °C, however, creep data allowing statements to be made about the stress dependence of the minimum creep rate or about the technically relevant creep strain limits are almost unavailable. This is not only due to reasons of time, but to technical reasons, too. In this stress-temperature range, the expected creep or strain rates are so small that they can hardly be measured by conventional creep tests. Therefore, a special long-term creep testing program at 550 °C and 600 °C, respectively, was started in 1991. After an experimental period of about 10 years the creep tests have been either finished or aborted, and evaluated [1,2]. Now, this low-stress creep data not only allow for a much better long-term prediction of the reliability of 316 L(N) applications but also enable deformation modeling for a broader stress range.

The according model has been derived from four different well-known deformation mechanisms [3-12] which are described by rate equations. It contains only four free parameters that have to be determined from experimental results.

Steady-State Creep Model

$$\dot{\gamma}_s = \dot{\gamma}_{sD} + \dot{\gamma}_{sP} + \begin{cases} \dot{\gamma}_{sPL} & for\ \ \sigma_s \le 86\,MPa \\ \dot{\gamma}_{sPLBD} & for\ \ \sigma_s > 86\,MPa \end{cases}$$

Creep by Diffusion

$$\dot{\gamma}_{sD} = 42\,\Omega\,\frac{1}{d^2}\,\frac{\sigma_s}{kT}\left(D_L + \frac{\pi\delta}{d} D_B\right) \quad \text{where} \quad D = D_0\,e^{-\frac{Q}{RT}}$$

Power-Law Creep

$$\dot{\gamma}_{sPL} = c_3\,\frac{\mu b}{kT}\left(\frac{\sigma_s}{\mu}\right)^n D_C \quad \text{where} \quad D_C = D_{0C}\,e^{-\frac{Q_C}{RT}}$$

Power-Law Breakdown

$$\dot{\gamma}_{sPLBD} = c_4\left[\sinh\left(\alpha'\frac{\sigma_s}{\mu}\right)\right]^n \exp\left[-\frac{Q_{cr}}{RT}\right]$$

Low Temperature Plasticity

$$\dot{\gamma}_{sP} = \dot{\gamma}_0 \exp\left[-\frac{Q_P}{RT}\left(1 - \frac{\sigma_s}{\hat{\tau}}\right)\right], \quad \hat{\tau} \approx \frac{\mu b}{l}, \quad \dot{\gamma}_0 \sim \nu_d\left(\frac{\sigma_s}{\mu}\right)^2 \approx 10^6\,\tfrac{1}{s}$$

Diffusion Coefficients

$D_{0L} = 37.5 \cdot 10^{-6}\,\frac{m^2}{s}$

$D_{0B} \approx 6 \cdot 10^{-6}\,\frac{m^2}{s}$ $\quad D_{0C} = 10^{-5}\,\frac{m^2}{s}$

Activation Energies

$Q_L = 280\,\frac{kJ}{mol}$ $\quad Q_P = 0.75\,\mu b^3$

$Q_B \approx 200\,\frac{kJ}{mol}$ $\quad Q_{cr} \equiv Q_C = 520\,\frac{kJ}{mol}$

Model Constants

$c_4 \equiv c_3 D_{0C}$ $\quad n \equiv 7$

$c_3 = 2 \cdot 10^{20}$ $\quad \alpha' = 800$

Material Constants

Atomic Volume	$\Omega \approx 1.2 \cdot 10^{-29}\,m^3$
Grain Size	$d \approx 100\,\mu m$
Thickness of Grain Boundary	$\delta \approx 20\,nm$
shear modulus	$\mu(T) = \mu_0\left(1 - 0.85\,\frac{T - 300K}{T_M}\right)$ $\mu_0 = 81000\,\frac{MN}{m^2}$
melting temperature	$T_M = 1810\,K$
Burger's vector	$b = \lvert\mathbf{b}\rvert = 2.85 \cdot 10^{-10}\,m$
obstacle spacing	$l \approx 40\,nm$

As can be seen, the transition from power-law creep to plasticity (which has been fitted just to the 600 °C results) fits also nicely to the results gained at 550 °C and 650 °C. At higher temperatures the experiments have been performed at stresses below the transition range.The power-law creep range which has been fitted to the 600 °C, 650 °C, and 700 °C experimental results, applies also for the 750 °C test results. Only the creep tests performed at 600 °C reach down to the range of diffusion creep. Therefore, it is not possible to verify the whole model for the other temperatures. But at least for 600 °C the model predictions fit perfectly to the experiments. At 550 °C, however, the model is too optimistic.

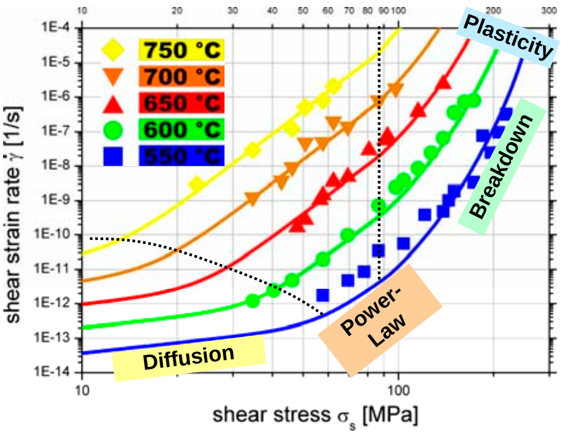

Fig.1: Creep model (lines) as defined above compared to the experimental results (symbols).

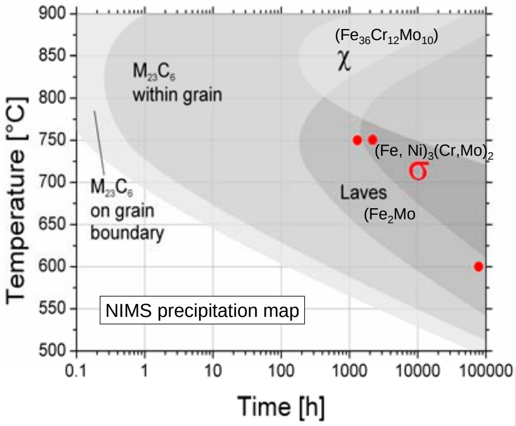

Fig.2: Precipitation map for AISI 316 L alloys [13] including sigma phase analysis for the present material (red dots).

For an evaluation of the influence of the time-dependent microstructural composition on the creep behavior a precipitation diagram is necessary. At NIMS, Japan extensive aging experiments have been performed followed by TEM examinations to generate a time-temperature-precipitation diagram for a 18Cr-12Ni-Mo steel that is comparable to the AISI 316 L(N) [13]. In Fig. 2 this precipitation map is shown together with some results of the 316 L(N) sigma phase observations (see also Fig. 3) which are in good agreement. It can be seen that during steady-state creep in the medium and low stress range (i.e. 750 °C, 500 h down to 550 °C, 50000 h) only carbides and Laves phase precipitate at grain boundaries and within the grains. Therefore, the change of microstructure with time can not be the reason for the observed creep behavior shown in Fig.1. In fact, the steady-state creep rate depends strongly on the underlying deformation mechanisms which in turn depend on the applied stress [14].

Literature

1. M. Schirra, Nucl. Eng. Design **188**, 381-384 (1999).
2. M. Schirra, Annual Meeting on Nuclear Technology, Aachen, Germany, 13.-15. May 1997.
3. H. J. Frost, and M. F. Ashby, *Deformation-mechanism Maps*, Pergamon Press, Oxford, 1982.
4. F. R. N. Nabarro, in: *Report on Conference on Strength of Solids*, Phys. Soc. of London, 75, 1948.
5. C. Herring, J. Appl. Phys. **21**, 437 (1950).
6. F. Garofalo, *Fundamentals of Creep and Creep-Rupture in Metals*, MacMillan, New York, 1965.
7. B. Chalmers, *Physical Metallurgy*, John Wiley, New York, 1959.
8. A. P. Greenough, Phil. Mag. **43**, 1075 (1953).
9. B. H. Alexander, M. H. Dawson, and H. P. Kling, J. Appl. Phys. **22**, 439 (1951).
10. J. Weertman, J. Mech. Phys. Solids **4**, 230 (1956).
11. J. Weertman, Trans. AIME **218**, 207 (1960).
12. J. Weertman, Trans. AIME **227**, 1475 (1963).
13. NRIM-Metallographic Atlas of Long-term Crept Materials No. M-2, National Research Institute for Metals, Tokyo, Japan, 2003.
14. M. Rieth, Scientific Reports, FZKA 7065, Forschungszentrum Karlsruhe, 2005.

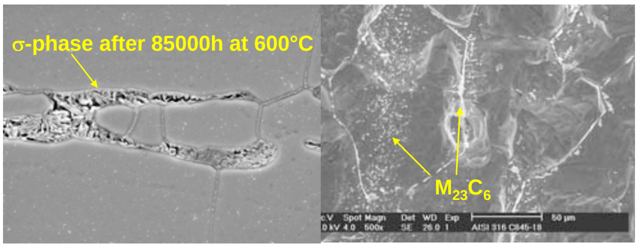

Fig.3: Sigma phase (left) and $M_{23}C_6$ precipitation (right) at and within grain boundaries.

18. August 2005